Bone 48 (2011) 1232–1238

Contents lists available at ScienceDirect

Bone

journal homepage: www.elsevier.com/locate/bone

Computational finite element bone mechanics accurately predicts mechanical competence in the human radius of an elderly population

Thomas L. Mueller [a], David Christen [a], Steve Sandercott [b], Steven K. Boyd [b], Bert van Rietbergen [c], Felix Eckstein [d], Eva-Maria Lochmüller [d], Ralph Müller [a], G. Harry van Lenthe [a,e,*]

[a] Institute for Biomechanics, ETH Zurich, Zurich, Switzerland
[b] Department of Mechanical and Manufacturing Engineering, Schulich School of Engineering, University of Calgary, Calgary, Canada
[c] Department of Biomedical Engineering, Eindhoven University of Technology, Eindhoven, The Netherlands
[d] Institute of Anatomy and Musculoskeletal Research, Paracelsus Medical University Salzburg, Salzburg, Austria
[e] Division of Biomechanics and Engineering Design, K.U. Leuven, Leuven, Belgium

ARTICLE INFO

Article history:
Received 11 August 2010
Revised 28 December 2010
Accepted 24 February 2011
Available online 2 March 2011

Edited by: Harry Genant

Keywords:
Human radius
High-resolution pQCT
Finite element analysis
Bone strength
Bone competence

ABSTRACT

High-resolution peripheral quantitative computed tomography (HR-pQCT) is clinically available today and provides a non-invasive measure of 3D bone geometry and micro-architecture with unprecedented detail. In combination with microarchitectural finite element (μFE) models it can be used to determine bone strength using a strain-based failure criterion. Yet, images from only a relatively small part of the radius are acquired and it is not known whether the region recommended for clinical measurements does predict forearm fracture load best. Furthermore, it is questionable whether the currently used failure criterion is optimal because of improvements in image resolution, changes in the clinically measured volume of interest, and because the failure criterion depends on the amount of bone present. Hence, we hypothesized that bone strength estimates would improve by measuring a region closer to the subchondral plate, and by defining a failure criterion that would be independent of the measured volume of interest. To answer our hypotheses, 20% of the distal forearm length from 100 cadaveric but intact human forearms was measured using HR-pQCT. μFE bone strength was analyzed for different subvolumes, as well as for the entire 20% of the distal radius length. Specifically, failure criteria were developed that provided accurate estimates of bone strength as assessed experimentally. It was shown that distal volumes were better in predicting bone strength than more proximal ones. Clinically speaking, this would argue to move the volume of interest for the HR-pQCT measurements even more distally than currently recommended by the manufacturer. Furthermore, new parameter settings using the strain-based failure criterion are presented providing better accuracy for bone strength estimates.

Introduction

Osteoporosis is recognized as a major public health problem worldwide, leading to reduced bone strength and an increase in fractures. Fractures in the region of the distal radius are among the most common in humans and their incidence is increasing due to the aging population. Osteoporosis reduces bone strength through a loss of bone mass and diminished structural integrity. Bone loss can be assessed easily and accurately with dual-energy X-ray absorptiometry (DXA) and was shown to correlate with mechanical strength and bone fracture risk [1,2]. For this reason, estimates of bone strength are nowadays typically based on areal bone mineral density (aBMD) measurements. However, aBMD is not a direct measure of bone strength and is not sufficient to predict bone strength in individual patients. It has been shown that predicting trabecular bone strength can be improved by including microarchitectural parameters in the analysis [3,4]. Indeed, the decrease in bone mass and the removal of structural elements have been shown to result in an increased fracture incidence [5,6]. Furthermore, distal radius volumetric BMD (vBMD) and microstructural indices better discriminated 35 postmenopausal women with mixed fractures from 78 postmenopausal women without fractures than aBMD of the hip or spine [7].

With the introduction of a new generation of high-resolution 3D peripheral quantitative computed tomography (HR-pQCT) systems, direct quantification of structural bone parameters has become possible in living patients. In addition, it is now possible to estimate

* Corresponding author at: Institute for Biomechanics, ETH Zurich, Wolfgang-Pauli-Str. 14, HPI F22, 8093 Zurich, Switzerland. Fax: +41 44 633 15 73.
E-mail addresses: tmueller@ethz.ch (T.L. Mueller), dchristen@ethz.ch (D. Christen), ssanderc@engmail.uwaterloo.ca (S. Sandercott), skboyd@ucalgary.ca (S.K. Boyd), B.v.Rietbergen@tue.nl (B. van Rietbergen), felix.eckstein@pmu.ac.at (F. Eckstein), Eva-Maria.Lochmueller@gmx.de (E.-M. Lochmüller), ram@ethz.ch (R. Müller), vanlenthe@ethz.ch (G.H. van Lenthe).

8756-3282/$ – see front matter © 2011 Elsevier Inc. All rights reserved.
doi:10.1016/j.bone.2011.02.022

bone strength directly using micro-finite element (μFE) analysis [8]. It was recently found that estimated load/strength ratios as assessed by μFE analysis at the ultradistal radius more closely simulated patterns of wrist fractures occurring in the same population than did measurements of vBMD [9]. Furthermore, in human cadaveric forearms good agreement was demonstrated between estimated bone strength as assessed by μFE analyses and those measured using mechanical testing [10]. The μFE estimated bone strength predicted the measured bone strength significantly better than bone densitometry [11]. The good predictive capability of μFE estimated bone strength was confirmed for more recent HR-pQCT systems that provide an improved nominal resolution of 82 μm. MacNeil and Boyd have also shown that both the experimentally and computationally determined bone stiffness are excellent predictors of bone strength [12]. Furthermore, the potential of HR-pQCT based μFE to identify people at risk of distal radius fracture has been demonstrated [13]. In addition, it has been shown that bone geometry, microstructure and strength contribute to forearm fractures in postmenopausal women, as does BMD, and that these additional determinants of risk promise greater insight into fracture pathogenesis [14]. Consequently, HR-pQCT provides a non-invasive and clinically useful measure of 3D micro-architecture at the distal radius, and these data are adequate to estimate bone strength using patient-specific finite element models.

Yet, images from only a relatively small part of the radius are acquired (9.02 mm field of view in axial direction) as recommended by the manufacturer for clinical measurements of the forearm. So far, no studies are available assessing bone strength in different measurement volumes of interest in a larger patient population. Furthermore, μFE bone strength estimates of former clinical studies were assessed using a failure criterion developed by Pistoia et al. [10]. Specifically, this criterion defines bone strength as the force at which 2% of the bone volume is strained above 0.7% effective strain. Due to improvements in image resolution and differences in the clinically measured volume of interest it is questionable if this criterion is still valid. Even more so, the dependency of the criterion on the measured bone volume is debatable. Therefore, two hypotheses were tested in this study. First, we hypothesized that regions with thinner cortices, hence, regions closer to the subchondral plate than currently recommended, would improve the bone strength prediction at the distal radius. We tested this hypothesis by using μFE predictions of estimated bone strength as well as by a visualization of the failure behavior using image-guided failure analysis (IGFA). Second, we hypothesized that the estimated bone strength would be improved when the criterion would be independent of the measured volume of interest. Acceptance of these hypotheses might influence future clinical studies, by which human radius bone strength estimations will be performed, a focus which has been developing quickly over the last years.

Methods

Specimens

A sample group of 163 embalmed human cadavers was investigated, from which results have been presented in different studies up to this date [2,15–18]. In line with German legislative requirements, the donors had dedicated their bodies to the Institute of Anatomy of the Ludwig-Maximilians-University (LMU) Munich prior to death. The intact forearms were detached at the distal humerus. Based on different exclusion criteria, as previously reported [18], the final sample included 50 males (age 79.9 ± 8.76 years) and 50 age-matched females (age 81.6 ± 8.86 years), hence, 100 specimens in total. Areal bone mineral density (aBMD) at the distal radius as assessed by peripheral dual-energy X-ray absorptiometry (DXA) was 0.37 ± 0.09 g/cm^2 for males and 0.24 ± 0.08 g/cm^2 for females, respectively.

Imaging

The forearms were imaged using an HR-pQCT scanner (a prototype of the XtremeCT, Scanco Medical AG, Brüttisellen, Switzerland) providing a nominal resolution of 89 μm in plane and 93 μm slice thickness. The X-ray tube was operated at 60 kVp. Image processing was performed according to the manufacturer's recommendations. Segmentation of the structure was carried out with a 3D Laplace–Hamming filter and a fixed global threshold for all samples [19]. Specifically, the Hamming cut-off frequency was 0.4 of the Nyquist frequency, the weighting factor 0.5 and the threshold 415/1000 of the maximal gray scale value. Since the cadaver arms were scanned with intact soft tissues, the images are representative for in vivo situations in living subjects, only lacking potential motion artifacts. Measurements were acquired in a volume of interest (VOI) starting at the distal joint, and covered more than 20% of the forearm length. Five consecutive VOIs, each with a width corresponding to 4% of the forearm length were defined, with VOI 1 starting proximal to the subchondral plate (Fig. 1). An additional VOI 1B was defined according to the manufacturer's recommendations for in vivo measurements. Finally, the five consecutive VOIs were also analyzed as one full bone region (VOI FB).

Mechanical testing

Ultimate failure load was assessed by uniaxial mechanical testing which was performed based on a protocol as previously reported by Lochmüller et al. [2]. The intact forearms were subjected to compression until complete fracture, using a Zwick 1445 (Ulm, Germany) system. The forces applied to the hand were similar in magnitude and direction to those that occur during a fall on the outstretched hand usually leading to a Colles-type fracture of the radius [1,2,16,20]. From the radiographs taken after testing, fractures were classified by an experienced musculoskeletal radiologist. For the 100 specimens, a detailed description of the distal forearm fracture types according to the Frykman classification has been presented [18]. Bone strength was defined as the peak of the force displacement curve, followed by a drop in registered load to less than 70% of the peak value.

Microstructural finite element analysis

μFE models of the full bone (VOI FB) and of the six single VOIs were created by a direct conversion of bone voxels to cubic hexahedral elements. A custom-built in-house mesher was used to generate the FE meshes. Meshing was performed on 8 dual-core 2.6 GHz AMD Opteron processors of a Cray XT3 system at the Swiss National Supercomputing Centre (CSCS, Manno, Switzerland). Linear and isotropic material behavior was assumed; Young's modulus (E) and Poisson's ratio (ν) were 6.829 GPa and 0.3 respectively [12]. The

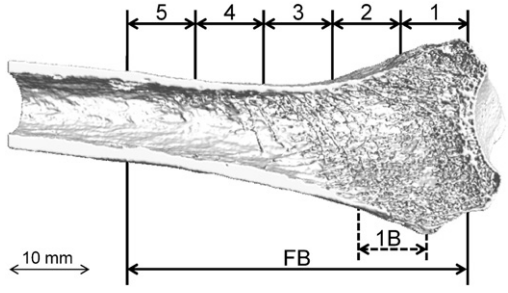

Fig. 1. 3D image as assessed by high-resolution peripheral quantitative computed tomography (HR-pQCT) of a 92 year old female human radius. Analyses were performed in five subsequent VOIs each covering 4% of the radius length. The sixth VOI (1B), which corresponds to the recommended scan VOI, was analyzed. VOI FB consists of the five subsequent single VOIs.

boundary conditions represented the experimental uniaxial compression tests. Nodes at the top surface (distal side) were free to move in the transversal plane while a prescribed displacement in axial direction was applied corresponding to 1% apparent strain. All nodes on the bottom platen surface (proximal side) of the models were fixed in the direction of the displacement (i.e. uniaxial testing direction), except for two nodes which were restricted in the transversal plane in order to prevent rigid body rotation and translations. For the solution of these models with up to 80 million degrees of freedom, a parallel linear finite element package (ParFE) with an algebraic multigrid preconditioner was used [21]. The models were processed on a Cray XT3 system on 256 dual-core 2.6 AMD Opteron processors. Solving time per single VOI model was between two and four minutes. The force required to reach 1% apparent strain was calculated as were the tissue-level stresses and strains. Visualizations were created in parallel using the open source program ParaView (http://www.paraview.org/) on 4 AMD Opteron CPU nodes with a total of 32 GB of memory on a HP-XC cluster.

Failure criterion to estimate μFE bone strength

In the μFE models, failure was expected to occur as soon as the effective strain levels in a characteristic fraction of the bone volume exceeded a certain critical threshold. In the original formulation by Pistoia et al. [10] the characteristic bone volume fraction (V_{crit}) was set to 2%, the Young's modulus (E) to 10 GPa, the Poisson's ratio (ν) to 0.3 and the effective strain threshold to 0.7%. These values were derived for a pQCT system providing a resolution of 165 μm. It is not known whether V_{crit} depends on image resolution; hence, a V_{crit} of 2% may not provide the best estimate in the present study because we used a more recent, higher resolution scanner providing an improved level of detail. Furthermore, the optimal V_{crit} may depend on boundary conditions and material properties. For that purpose we ran analyses to quantify how V_{crit} affected bone strength estimates. Specifically, we expressed the critical volume in relative numbers ($V_{crit\text{-}\%}$) similar to the original definition. $V_{crit\text{-}\%}$ was varied between 0.1% and 1.0% in steps of 0.1%, between 1.0% and 10.0% in steps of 0.5% and between 10.0% and 95.0% in steps of 5.0%, respectively. Additionally, critical volume was expressed in absolute numbers ($V_{crit\text{-}mm^3}$) as to gain a criterion which is independent of the measured volume of interest. $V_{crit\text{-}mm^3}$ was analyzed in steps of 10 mm^3 starting with 1 mm^3 to 300 mm^3. For each set of parameters the estimated μFE bone strength of all 100 specimens was correlated to the measured bone strength as a linear regression analysis. The discrepancy between μFE estimated bone strength and experimentally measured bone strength was expressed by the root-mean-square errors (RMSE).

Image guided failure assessment (IGFA)

Using image-guided failure assessment (IGFA) [22–25] the mechanism of failure at the human distal radius under compressive loading was characterized. Five left fresh human cadaver radii (53 to 90 years) were investigated (Gross Anatomy Laboratory, University of Calgary), and the distal 120 mm of the radii were excised for IGFA. A custom IGFA device was built for the HR-pQCT that can apply axial, torsional or combined loads [26]. The radii were tested to failure in compression by applying a maximum of 3% apparent strain in steps of 0.375% of the total length. The proximal end of the radius was embedded in PMMA, and the distal end of the joint was pressed into a PMMA mold during compression. For all specimens and loading steps, 3D images of the distal 40 mm were acquired by HR-pQCT (XtremeCT, Scanco Medical AG, Brüttisellen, Switzerland; 82 μm isotropic voxel) and the sequential visualizations of the bone under load were used to generate animated visualizations. Axial loads and displacements in the IGFA were recorded throughout the loading and imaging protocol. All procedures were approved by the Office of Medical Bioethics at the University of Calgary.

Statistics

Descriptive statistics were computed for μFE indices at each of the 7 different VOIs. The experimentally measured bone strength was linearly related to the μFE analyzed bone strength and the coefficient of determination (r^2) based on the Pearson product-moment correlation coefficient was computed. Furthermore, root mean square errors (RMSE) were analyzed to determine the failure criterion with the best accuracy between estimated and measured bone strength. Finally, multiple linear regression was used to demonstrate whether one region or one failure criterion added significant information. Statistical analyses were performed with Excel 2007 (Microsoft, Redmond, USA) and R version 2.7.2 (The R Foundation for Statistical Computing).

Results

The tissue-level stresses and strains were calculated for all VOIs. Marked differences in strain distribution were found when going from the most distal VOI to more proximal ones (Fig. 2). RMSE values depended strongly on V_{crit} (Fig. 3). For all VOIs an optimal V_{crit} could be found that minimized RMSE. Smallest RMSE values were found for VOI FB, and were closely followed by the distal VOIs. The minimal RMSE values, either expressed in absolute or relative terms, differed strongly for the different VOIs, hence, for different bone microstructures. Table 1 lists the optimal failure criterion parameters for all VOIs that minimized RMSE as well as the corresponding linear correlation coefficients r^2. Furthermore, RMSE and correlation coefficients are shown for the standard failure criterion by Pistoia et al. We found that RMSE as assessed by the original formulation were always higher (i.e. less accurate) than the one analyzed using our new parameter settings.

The μFE models from all VOIs could predict the average measured bone strength, as well as the standard deviations in a similar fashion (Fig. 4). No statistically significant differences were found between

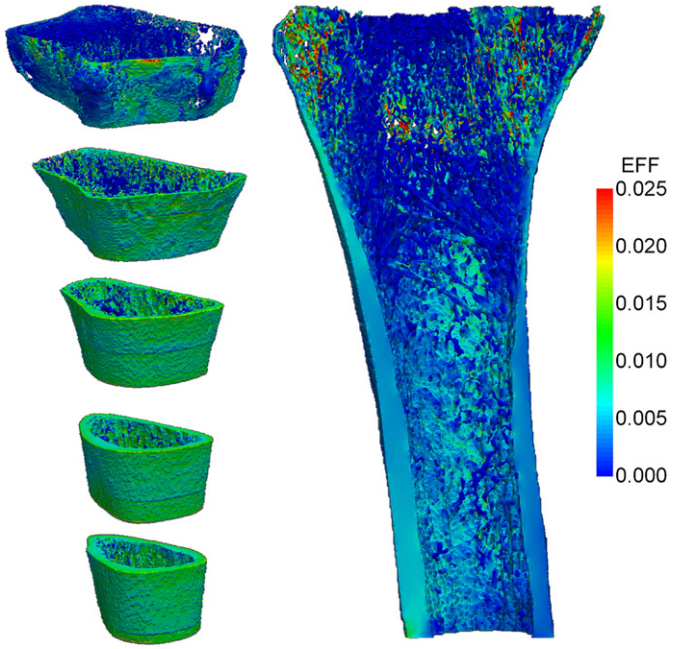

Fig. 2. Finite element analyses of five single VOIs as well as VOI FB. Results show the effective strain (EFF) distribution throughout the structure. Models consisted of up to 80 million degrees of freedom.

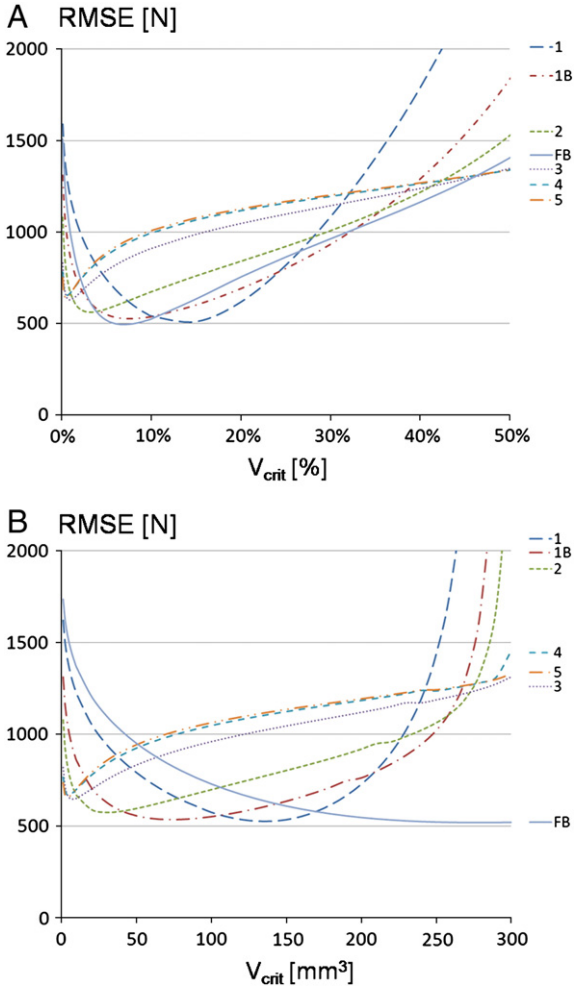

Fig. 3. The root-mean-square-error between estimated bone strength and experimentally measured bone strength as a function of the critical bone volume either expressed in a relative number (A) or in an absolute volume (B).

the experimentally measured and the μFE estimated bone strength. Nevertheless, when applying the criterion by Pistoia et al. one found a significant underestimation for VOI 1 and a significant overestimation in more proximal VOIs.

Table 1
RMSE and linear correlation coefficients between estimated and measured bone strength as assessed by the Pistoia criterion at a critical bone volume of 2%, an effective strain threshold of 0.7% and a Young's modulus of 10 GPa. The critical bone volume (V_{crit}) per volume of interest (VOI) that minimized the root-mean-square-error between estimated and experimentally measured bone strength assuming an effective strain threshold of 0.7% are shown in the second and third columns; linear correlation coefficients r^2 are presented, too; linear models were highly significant for all VOIs as well as for the different criterions with p-values<0.001.

	Criterion by Pistoia et al.			Optimal critical volume					
				$V_{crit-\%}$			$V_{crit-mm^3}$		
VOI	V_{crit} [%]	RMSE [N]	r^2	V_{crit} [%]	RMSE [N]	r^2	V_{crit} [mm^3]	RMSE [N]	r^2
1	2.0	571	0.76	15.0	511	0.78	140	526	0.74
1B	2.0	698	0.73	7.5	527	0.73	70	536	0.72
2	2.0	1065	0.69	3.0	562	0.69	30	573	0.69
3	2.0	1572	0.62	0.9	629	0.62	7	646	0.62
4	2.0	1725	0.60	0.6	654	0.60	5	670	0.60
5	2.0	1775	0.63	0.5	639	0.62	4	656	0.63
FB	2.0	561	0.78	7.0	496	0.76	280	520	0.76

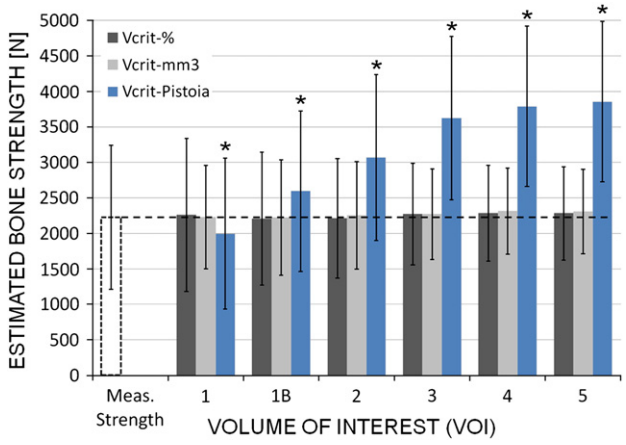

Fig. 4. Mean values and standard deviations of the measured bone strength as well as the μFE estimated bone strengths for the different VOIs, respectively. For all VOIs, bone strength was estimated at the optimal (minimized RMSE) critical bone volume strained beyond the yield strain. Additionally, bone strength was estimated for all VOIs using the criterion by Pistoia et al. The estimated bone strength using the Pistoia criterion differed significantly (*, $p<0.001$) from the measured bone strength, whereas no significant differences were found for the other criteria.

Accurate predictions of measured bone strength were achieved. Linear models for the different VOIs and criteria were highly significant for all tests. The best linear prediction of the measured bone strength using estimated bone strength was obtained at the most distal VOI (RMSE = 511 N, $r^2 = 0.78$; Table 1) with predictions decreasing towards more proximal VOIs (VOI 4, RMSE = 654 N, $r^2 = 0.60$).

Using multiple linear regression analysis including different VOIs (criterion $V_{crit-\%}$) we found that VOI 1 provided the most significant fraction ($p<0.001$); VOI 4 ($p<0.05$) and VOI 5 ($p<0.01$) provided less but still significant fractions. The multiple linear model including these 3 VOIs resulted in a coefficient of determination r^2 of 0.80. All other VOIs did not add significance to the linear model.

A multiple linear regression model of VOI 1 using the three different criteria showed that only the $V_{crit-\%}$ criterion had a significant effect on the model. The analysis of variance revealed significant differences between VOI 1 and VOI 1B. The interaction term was significant ($p = 0.038$) between $V_{crit-\%}$ estimated bone strength of VOI 1 and VOI 1B.

VOI FB, consisting of five consecutive single VOIs, predicted measured bone strength with almost the same accuracy as VOI 1 with a coefficient of determination of $r^2 = 0.76$. The estimated bone strength of VOI FB correlated extremely well with that of VOI 1 ($r^2 = 0.93$), VOI 1B ($r^2 = 0.98$), VOI 2 ($r^2 = 0.97$), VOI 3 ($r^2 = 0.90$), VOI 4 ($r^2 = 0.86$) and VOI 5 ($r^2 = 0.83$), indicating that single VOI analysis of bone strength is sufficient and only little additional information can be gained when analyzing a larger VOI (Fig. 5).

Finally, image-guided failure assessment of the five specimens showed consistent failure characterized by the collapse of the ultra-distal radius (VOI 1). The radii failed under axial compression at a mean load of 1885 N and a mean apparent strain of 2.1%. A radius under compression steps of 2.25% and 3.00% apparent strain is shown in Fig. 6A. Furthermore, Fig. 6B shows one representative force-displacement curve recorded during IGFA testing.

Discussion

The first hypothesis that regions closer to the subchondral plate would improve the bone strength prediction at the distal radius compared to the recommended measurement region was accepted. When investigating the strengths of the associations between the estimated and the measured bone strength, VOI 1 best predicted

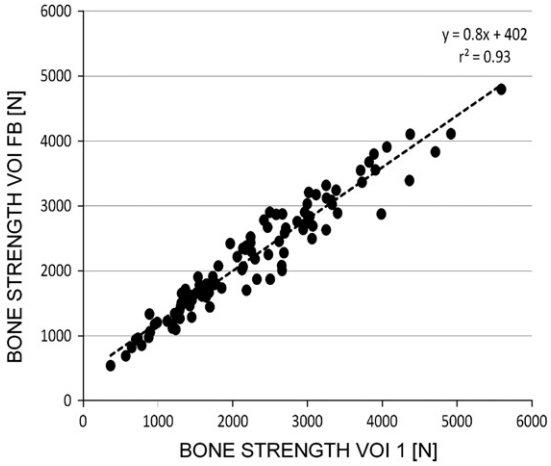

Fig. 5. VOI FB did correlate highly with VOI 1 and did not improve the failure load prediction ($r^2 = 0.93$).

measured bone strength (RMSE = 511 N) with RMSE increasing and correlation coefficients decreasing towards more proximal VOIs (Table 1). VOI 1B, recommended by the manufacturer, resulted in an increased RMSE and a lower correlation coefficient ($r^2 = 0.73$, while $r^2 = 0.78$ for VOI 1). This is not unexpected as the bone structure in VOI 1 seems to be weaker and less resistant to failure than in any other VOI. This finding was corroborated by our IGFA analyses, visually demonstrating that failure under compressive loading of the radius occurs in the most distal VOI. Moreover, Mueller et al. [18] have recently published data on

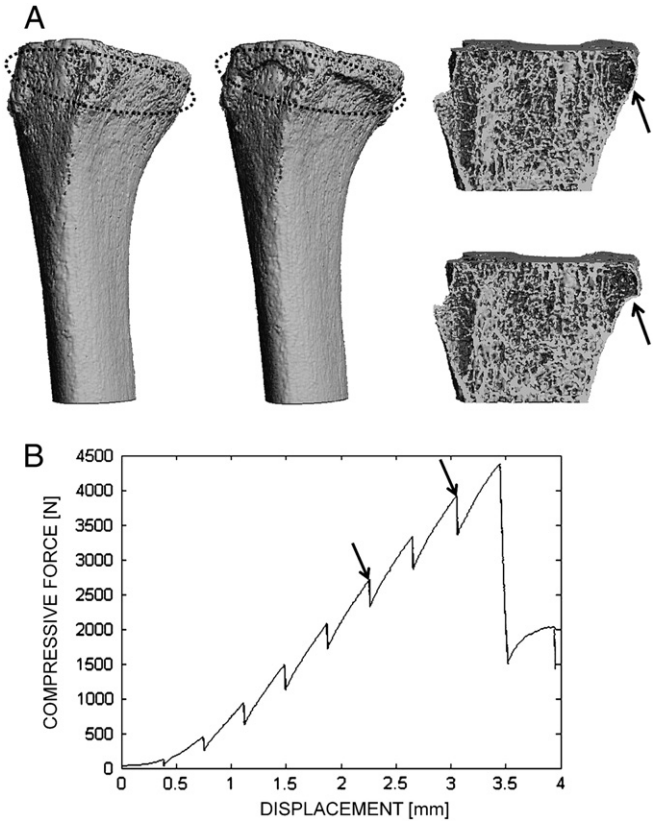

Fig. 6. (A) Two steps (of a total of 9) of a deformed radius under axial compression during image-guided failure analysis (IGFA); strain values were 2.25% and 3.00%. Bone failure occurred in the ultra-distal region. The left side represents the entire bone volume scanned during IGFA, and the right side corresponds to the same load steps and represents a cut-away of the ultradistal region during failure. (B) The load-displacement curve was measured during the IGFA experiment.

the comparison of morphological, DXA and anthropometric indices to bone strength data thereby showing that structural bone indices best predict failure in the most distal VOI 1, confirming the present findings. Interestingly, the large VOI FB did not improve the prediction of the measured bone strength when compared to the distal VOIs. One explanation for this was found in the fact that results from VOI FB correlated extremely well with those from single VOIs, indicating that only relatively little additional information for the analysis of bone strength can be gained from larger VOIs.

The second hypothesis that the analysis of estimated bone strength will be improved by using an absolute criterion which is independent of the measured volume of interest was rejected. Nevertheless, we showed that depending on the VOI different parameters have to be applied to achieve most accurate results (Table 1). Due to lower RMSE and higher correlation coefficients, especially at the more distal VOIs (Fig. 3, Table 1), we recommended to express critical bone volume as a percentage and not as an absolute value; specifically, we recommend a critical bone volume of 7.5% in combination with a strain threshold of 0.7% and a bone tissue modulus of 6.829 GPa for the currently clinically measured region corresponding to VOI 1B. If one would apply the failure criterion by Pistoia et al. the RMSE would be substantially increased by 32% even though the correlation coefficient would be identical. These results (Table 1) show clearly that depending on the measured VOI different parameter settings have to be chosen when using the failure criterion for bone strength analysis. Nevertheless, care should be taken to only apply these new values on HR-pQCT measurements with similar scanning settings and acquisition protocols, on this particular loading case for radius bone strength assessment and on the equivalent finite element method as it can be expected that the optimal parameters for this criterion will depend on image quality, image resolution, applied boundary conditions and material properties. Concerning former studies which used the failure criterion by Pistoia et al. at higher image resolution one can conclude that they provide good strength correlations even though the accuracy of estimated bone strength could have been improved by applying different parameter settings as presented here. Recently, Boutroy et al. [13] have adapted the parameter settings due to differences of the elastic properties they have used in their study, which were twice as high as those used by Pistoia et al. [10]. Nevertheless, these parameter adaptations were missing a thorough investigation and were solely applied to gain comparable failure loads. In summary, it is not needed that existing studies using the HR-pQCT derived μFE approach will have to be reanalyzed as the strength estimates are mainly affected in an absolute sense and correlations will be less affected. Nevertheless, in future studies we recommend to adapt to the here presented parameter settings for better accuracy.

A strength of our cadaver study was that we could measure a much larger part of the radius than measured in clinical studies. We covered 20% of the total forearm length and could therefore compare different axial VOIs. Furthermore, the biomechanical testing data on 100 human forearms is also unique and allowed the correlation of the estimated bone strength with the actual bone strength of the intact distal radius. It was shown that distal VOIs of the radius were more accurate in predicting bone strength than more proximal ones. Furthermore it was shown that, compared to DXA or structural parameters alone [18], μFE estimated bone strength is not only a directly comparable measure but can also lead to an improved estimation of bone strength ($r^2_{\mu FE} = 0.78$, $r^2_{architecture} = 0.74$, $r^2_{DXA} = 0.52$–0.71, respectively).

Clinically speaking, this would argue for moving the VOI for the HR-pQCT measurements even more distally than currently recommended by the manufacturer. Nevertheless, it also has to be considered that for example the responsiveness on therapies might be different in more proximal regions compared to the distal ones due to the thicker cortical bone and less trabecular structures. Therefore one has to take care in moving the region of interest more distally, thereby losing information on the more proximal structures.

Especially when analyzing longitudinal studies, one should consider measuring the ultra-distal as well as a more proximal region to include additional bone strength data on the bone therapy response, even though an additional radiation dose is needed. Finally, more studies are needed to confirm our results before such a recommendation could be implemented as this would have wide reaching consequences for currently ongoing clinical studies.

Another limitation of this study was that formalin fixed cadaver specimens were used. It is known that the formalin fixation can have some small effect on mechanical properties [27]. Therefore, biomechanical test results might not be entirely representative of bone strength in a living individual. Nevertheless, it is unlikely that the fixation had a major impact on the correlations investigated in these samples. It has to be noted that the laboratory based biomechanical measures do not fully represent human subject falling. There are other factors such as falling configuration and ground properties which are not considered in our experiment.

The second limitation is that we measured cadaver forearms, which may have limited some sources of error as compared to in vivo measurements, such as movement artifacts and physical positioning. Although in an ideal patient scanning scenario there will be no movement artifacts some caution may be required when applying the result of this study in an in vivo setting.

Another limitation of our study is that we used linear μFE analyses to model bone failure which is a time-dependent, nonlinear event including high local deformations and ultimate fractures. Although some work on bone failure characteristics has been done, at present, no standardized algorithms exist for assessing fracture from FE analyses; the precise failure mechanisms and associated material properties are still not well understood [8]. Nevertheless, this pragmatic approach to estimate strength from a single linear analysis has been successful [10]. Here we followed a similar approach, but in view of the different image resolution as well as due to differences in bone microstructure across the VOI under investigation, we ran analyses to quantify how V_{crit} affected bone strength estimates. Recently, MacNeil and Boyd have found excellent correlations between experimental bone strength and computationally determined stiffness [12]. Similar to our study, they have estimated bone strength in different VOIs. Different to our study was their mechanical test setup, with single VOIs being separately tested and therefore boundary conditions being similar to the ones applied in the μFE analysis. Moreover, Varga et al. have recently presented numerical results as assessed by a HR-pQCT-based anatomy specific FE technique showing good prediction for experimental stiffness and even better for strength [28]. They used excised cadaver radii rather than the intact forearm tests performed in this study. Therefore, it is not surprising that the predictive abilities in these two publications were higher than in our present study, where bone strength was determined from mechanical testing of intact forearms.

In summary, we found that the most relevant VOI to determine bone strength is located just below the subchondral plate. This finding was visually supported by IGFA testing. Good correlations and low RMSE between μFE derived bone strength and measured bone strength were demonstrated, especially in the most distal VOI. We determined the optimal parameters with which bone strength at the distal radius can be predicted from linear-elastic image-based models; these parameters depend on the specific volume of interest under investigation. For future studies, assessing radius bone strength by means of the HR-pQCT based linear μFE approach, we recommend using the parameter settings as determined in this study for better accuracy in bone strength estimates. We could not show that a VOI independent failure criterion would improve bone strength predictions. Our findings indicate that in vivo HR-pQCT derived μFE analysis is a promising way to assess bone strength in the human radius in patient populations. The presented results will improve clinical studies in which human radius bone strength estimations are performed, a focus which has been developing quickly over the last years.

Acknowledgments

This work was supported in part by the AO Foundation (network grant CPP1) and Swiss National Science Foundation (FP 620-58097.99). Computational time was granted by the Swiss National Supercomputing Centre (CSCS).

Appendix A. Supplementary data

Supplementary data to this article can be found online at doi:10.1016/j.bone.2011.02.022.

References

[1] Hudelmaier M, Kuhn V, Lochmüller EM, Well H, Priemel M, Link TM, et al. Can geometry-based parameters from pQCT and material parameters from quantitative ultrasound (QUS) improve the prediction of radial bone strength over that by bone mass (DXA)? Osteoporos Int 2004;15:375–81.
[2] Lochmüller EM, Kristin J, Matsuura M, Kuhn V, Hudelmaier M, Link TM, et al. Measurement of trabecular bone microstructure does not improve prediction of mechanical failure loads at the distal radius compared with bone mass alone. Calcif Tissue Int 2008;83:293–9.
[3] Müller R, Hannan M, Smith SY, Bauss F. Intermittent ibandronate preserves bone quality and bone strength in the lumbar spine after 16 months of treatment in the ovariectomized cynomolgus monkey. J Bone Miner Res 2004;19:1787–96.
[4] Turner CH, Cowin SC, Rho JY, Ashman RB, Rice JC. The fabric dependence of the orthotropic elastic constants of cancellous bone. J Biomech 1990;23:549–61.
[5] Kleerekoper M, Villanueva AR, Stanciu J, Rao DS, Parfitt AM. The role of three-dimensional trabecular microstructure in the pathogenesis of vertebral compression fractures. Calcif Tissue Int 1985;37:594–7.
[6] Mosekilde L, Mosekilde L, Danielsen CC. Biomechanical competence of vertebral trabecular bone in relation to ash density and age in normal individuals. Bone 1987;8:79–85.
[7] Boutroy S, Bouxsein ML, Munoz F, Delmas PD. In vivo assessment of trabecular bone microarchitecture by high-resolution peripheral quantitative computed tomography. J Clin Endocrinol Metab 2005;90:6508–15.
[8] van Lenthe GH, Müller R. Prediction of failure load using micro-finite element analysis models: toward in vivo strength assessment. Drug Discov Today Technol 2006;3:221–9.
[9] Riggs BL, Melton III LJ, Robb RA, Camp JJ, Atkinson EJ, Oberg AL, et al. Population-based analysis of the relationship of whole bone strength indices and fall-related loads to age- and sex-specific patterns of hip and wrist fractures. J Bone Miner Res 2006;21:315–23.
[10] Pistoia W, van Rietbergen B, Lochmüller EM, Lill CA, Eckstein F, Rüegsegger P. Estimation of distal radius failure load with micro-finite element analysis models based on three-dimensional peripheral quantitative computed tomography images. Bone 2002;30:842–8.
[11] Pistoia W, van Rietbergen B, Lochmüller EM, Lill CA, Eckstein F, Rüegsegger P. Image-based micro-finite-element modeling for improved distal radius strength diagnosis: moving from bench to bedside. J Clin Densitom 2004;7:153–60.
[12] MacNeil JA, Boyd SK. Bone strength at the distal radius can be estimated from high-resolution peripheral quantitative computed tomography and the finite element method. Bone 2008;42:1203–13.
[13] Boutroy S, Van Rietbergen B, Sornay-Rendu E, Munoz F, Bouxsein ML, Delmas PD. Finite element analysis based on in vivo HR-pQCT images of the distal radius is associated with wrist fracture in postmenopausal women. J Bone Miner Res 2008;23:392–9.
[14] Melton III LJ, Riggs BL, van Lenthe GH, Achenbach SJ, Müller R, Bouxsein ML, et al. Contribution of in vivo structural measurements and load/strength ratios to the determination of forearm fracture risk in postmenopausal women. J Bone Miner Res 2007;22:1442–8.
[15] Eckstein F, Matsuura M, Kuhn V, Priemel M, Müller R, Link TM, et al. Sex differences of human trabecular bone microstructure in aging are site-dependent. J Bone Miner Res 2007;22:817–24.
[16] Hudelmaier M, Kollstedt A, Lochmüller EM, Kuhn V, Eckstein F, Link TM. Gender differences in trabecular bone architecture of the distal radius assessed with magnetic resonance imaging and implications for mechanical competence. Osteoporos Int 2005;16:1124–33.
[17] Lochmüller EM, Matsuura M, Bauer J, Hitzl W, Link TM, Müller R, et al. Site-specific deterioration of trabecular bone architecture in men and women with advancing age. J Bone Miner Res 2008;23:1964–73.
[18] Mueller TL, van Lenthe GH, Stauber M, Gratzke C, Eckstein F, Muller R. Regional, age and gender differences in architectural measures of bone quality and their correlation to bone mechanical competence in the human radius of an elderly population. Bone 2009;45:882–91.

[19] Laib A, Rüegsegger P. Comparison of structure extraction methods for in vivo trabecular bone measurements. Comput Med Imaging Graph 1999;23:69–74.
[20] Metz S, Kuhn V, Kettler M, Hudelmaier M, Bonel HM, Waldt S, et al. Comparison of different radiography systems in an experimental study for detection of forearm fractures and evaluation of the Muller-AO and Frykman classification for distal radius fractures. Invest Radiol 2006;41:681–90.
[21] Arbenz P, van Lenthe GH, Mennel U, Müller R, Sala M. A scalable multi-level preconditioner for matrix-free μ-finite element analysis of human bone structures. Int J Numer Methods Eng 2008;73:927–47.
[22] Hulme PA, Ferguson SJ, Boyd SK. Determination of vertebral endplate deformation under load using micro-computed tomography. J Biomech 2008;41:78–85.
[23] Müller R, van Lenthe GH. Trabecular bone failure at the microstructural level. Curr Osteoporos Rep 2006;4:80–6.
[24] Nazarian A, Müller R. Time-lapsed microstructural imaging of bone failure behavior. J Biomech 2004;37:55–65.
[25] Nazarian A, Stauber M, Müller R. Design and implementation of a novel mechanical testing system for cellular solids. J Biomed Mater Res B Appl Biomater 2005;73:400–11.
[26] Sandercott SD, Hofmann M, Boucousis S, Dumont J, Müller R, Boyd SK. Fracture of the human distal radius in compression and torsion by image guided failure analysis and HR-pQCT. 18th International Bone Densitometry Workshop, Foggia, Italy; 2008. p. 76.
[27] Lochmüller EM, Krefting N, Burklein D, Eckstein F. Effect of fixation, soft-tissues, and scan projection on bone mineral measurements with dual energy X-ray absorptiometry (DXA). Calcif Tissue Int 2001;68:140–5.
[28] Varga P, Baumbach S, Pahr D, Zysset PK. Validation of an anatomy specific finite element model of Colles' fracture. J Biomech 2009;42:1726–31.